**Supporting Information**

# Adsorption of phosphate and cadmium on iron (oxyhydr)oxides: A comparative study on ferrihydrite, goethite, and hematite

Jing Liu[1], Runliang Zhu[1]*, Lingya Ma[1], Haoyang Fu[1,2], Xiaoju Lin[1,2], Stephen C. Parker[3], Marco Molinari[3,4]

1. *CAS Key Laboratory of Mineralogy and Metallogeny/Guangdong Provincial Key Laboratory of Mineral Physics and Materials, Guangzhou Institute of Geochemistry, Chinese Academy of Sciences (CAS), Guangzhou 510640, China*
2. *University of Chinese Academy of Sciences, Beijing 100049, China; Institutions of Earth Science, Chinese Academy of Sciences, Beijing 100029, China*
3. *Department of Chemistry, University of Bath, Claverton Down, Bath, BA2 7AY, UK*
4. *Department of Chemistry, University of Huddersfield, Queensgate, Huddersfield HD1 3DH, United King*

* Corresponding author

Phone: 86-020-85297603

Fax: 86-020-85297603

E-mail: zhurl@gig.ac.cn

The supporting information includes 1 table and 3 figures:

**Table S1.** The removal rates of phosphate and cadmium in the adsorption isotherms in ternary systems.

**Table S2**. The Freundlich isotherm constants for the adsorption of phosphate on Fh, Gt, and Hm.

**Table S3**. The removal efficiencies of phosphate and cadmium in the pH envelopes in ternary systems.

**Table S4.** the saturation index of the possible precipitations in ternary systems calculated using Visual Minteq 3.1.

**Fig. S1**. The $N_2$ adsorption-desorption isotherms of Fh, Gt, and Hm.

**S1** Introduction of two-dimensional correlation spectroscopy.

**Fig. S2.** Adsorption isotherms of phosphate (A) and cadmium (B) in the binary adsorption systems on Fh, Gt, and Hm.

**Fig. S3.** Synchronous (the figures filled with the red) and asynchronous spectra (the figures filled with red and blue) of phosphate complexes on goethite in the binary (A) and ternary adsorption systems (B).

**Fig. S4.** Synchronous and asynchronous spectra of hematite in the single (A) and double solutes adsorption systems (B).

**Fig. S5.** Synchronous and asynchronous spectra of phosphate on ferrihydrite in the binary (A) and ternary adsorption systems (B).

Table S1. The removal efficiencies of phosphate and cadmium in the adsorption isotherms in ternary systems.

| Initial concentration of phosphate and Cd (mM) | Removal efficiencies | | | | | |
|---|---|---|---|---|---|---|
| | Phosphate | | | cadmium | | |
| | Fh | Gt | Hm | Fh | Gt | Hm |
| 0.125 | 0.92 | 0.99 | 1.00 | 0.40 | 0.11 | 0.18 |
| 0.25 | 0.78 | 1.00 | 0.99 | 0.47 | 0.13 | 0.16 |
| 0.40 | 0.72 | 0.87 | 0.95 | 0.44 | 0.18 | 0.22 |
| 0.60 | 0.53 | 0.67 | 0.81 | 0.40 | 0.25 | 0.28 |
| 0.80 | 0.41 | 0.47 | 0.68 | 0.40 | 0.31 | 0.26 |
| 1.00 | 0.36 | 0.34 | 0.58 | 0.42 | 0.29 | 0.28 |
| 1.50 | 0.36 | 0.19 | 0.45 | 0.37 | 0.29 | 0.24 |
| 2.00 | 0.34 | 0.13 | 0.37 | 0.35 | 0.25 | 0.19 |

Table S2. The Freundlich isotherm constants for the adsorption of phosphate on Fh, Gt, and Hm.

| Minerals | Freundlich constants | | |
|---|---|---|---|
| | K | n | $R^2$ |
| Fh | 0.574 | 9.52381 | 0.89 |
| Gt | 0.11847 | 7.694083 | 0.96 |
| Hm | 0.0452 | 7.363228 | 0.79 |

Table S3. The removal efficiencies of phosphate and cadmium in the pH envelopes in ternary systems.

| No. (from the lowest to highest pH values in each system) | Removal efficiencies | | | | | |
|---|---|---|---|---|---|---|
| | Phosphate | | | Cadmium | | |
| | Fh | Gt | Hm | Fh | Gt | Hm |
| 1 | 0.90 | 0.86 | 0.82 | 0.13 | 0.11 | 0.08 |
| 2 | 0.87 | 0.86 | 0.81 | 0.18 | 0.15 | 0.09 |
| 3 | 0.87 | 0.86 | 0.81 | 0.24 | 0.20 | 0.11 |
| 4 | 0.87 | 0.85 | 0.81 | 0.27 | 0.28 | 0.19 |
| 5 | 0.87 | 0.86 | 0.82 | 0.35 | 0.36 | 0.24 |
| 6 | 0.85 | 0.86 | 0.82 | 0.38 | 0.41 | 0.29 |
| 7 | 0.87 | 0.87 | 0.82 | 0.44 | 0.45 | 0.35 |
| 8 | 0.88 | 0.87 | 0.84 | 0.49 | 0.49 | 0.40 |
| 9 | 0.87 | 0.87 | 0.84 | 0.64 | 0.51 | 0.41 |
| 10 | 0.88 | 0.89 | 0.85 | 0.70 | 0.61 | 0.46 |

Table S4. the saturation index of the possible precipitations in ternary systems calculated using Visual Minteq 3.1 (0.6 mM phosphate and cadmium, 0.4 g/L Fh, 2.5 g/L Gt, and 4 g/L Hm, pH 6.5). The complexation parameters for Fh and Gt are available in the software. Parameters for ferrihydrite are from Tiberg and Gustafsson, (2016), and for goethite are from Weng et al., (2001). The parameters for Hm are from (Christl and Kretzschmar, 1999; Komárek et al., 2018).

| Minerals | Saturation index (=logIAP-logKs) | |
|---|---|---|
| | $Cd(OH)_2$ | $Cd_3(PO_4)_2$ |
| Fh | -4.416 | -1.437 |
| Gt | -4.449 | -0.865 |
| Hm | -4.627 | -0.271 |

Fig. S1 The $N_2$ adsorption-desorption isotherms of Fh, Gt, and Hm.

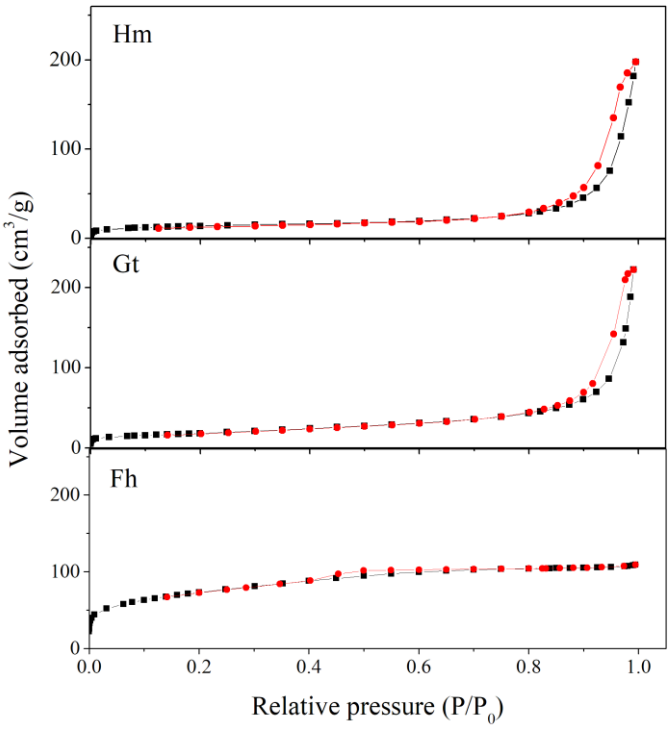

**Introduction of two-dimensional correlation spectroscopy (2D-COS)**

The 2D-COS is performed according to the theory of Noda. A set of one-dimensional spectra collected under external perturbation (e.g., time, concentration, pH) is transformed into a 2D correlation spectrum, which consists of two orthogonal components: synchronous and asynchronous plots. The former represents the simultaneous or coincidental changes of two separate spectral intensity variations during the interval, while the latter represents out-of-phase changes.

The synchronous plot is symmetric concerning the diagonal and including diagonal peaks (auto peaks) and off-diagonal peaks (cross peaks). The auto peaks are always positive and reveal the significant changes in spectral intensities during the perturbation. Thus, any region of a spectrum which changes the intensity to a great extent under perturbation will show strong autopeaks, while those remaining near constants develop little or no autopeaks. Cross-peaks can be positive (when intensities at two separate wavenumbers increase or decrease simultaneously) or negative (when the increase in intensity at one wavenumber is coupled to the decrease in intensity at another wavenumber).

Unlike the synchronous plot, the asynchronous plot is asymmetric with respect to the diagonal line and consists exclusively of cross peaks, which develops only if the intensities of two spectral features change out of phase with each other. This feature is very useful in enhancing the resolution and separating the overlapped bands arising from different species. On the other hand, the sequential order of intensity changes between two bands at $\nu_1$ and $\nu_2$ could also be obtained from the sign of synchronous correlation peak $\Phi(\nu_1, \nu_2)$ and asynchronous correlation peak $\Psi(\nu_1, \nu_2)$ according to the well-established principles. In brief, when $\Phi(\nu_1, \nu_2)$ and $\Psi(\nu_1, \nu_2)$ have the same sign, the change in the spectral intensity at $\nu_1$ band occurs prior to that at $\nu_2$, while the order is reversed if $\Phi(\nu_1, \nu_2)$ and $\Psi(\nu_1, \nu_2)$ have the opposite sign. The changes at $\nu_1$ and $\nu_2$ occur simultaneously if $\Psi(\nu_1, \nu_2)$ is zero. Thus, the sequential order of different species could also be speculated based on the sequential order of different bands.

In this study, the collected time-resolved spectra were subjected to the 2D

correlation analysis using the 2Dshige code (https://sites.google.com/site/shigemorita/home/2dshige.). From inspection of the regular spectra, we believe that the peaks below 880 and above 1160 $cm^{-1}$ in the phosphate spectra are caused by baseline changes in this region and will not be further discussed since the asynchronous plot is sensitive to all changes in the spectra including baseline or noise.

Fig. S2. Adsorption isotherms of phosphate (A) and cadmium (B) in the binary adsorption systems on Fh, Gt, and Hm (the grey and black dashed lines in Fig. A are the fitted adsorption isotherms using Langmuir and Freundlich models, respectively).

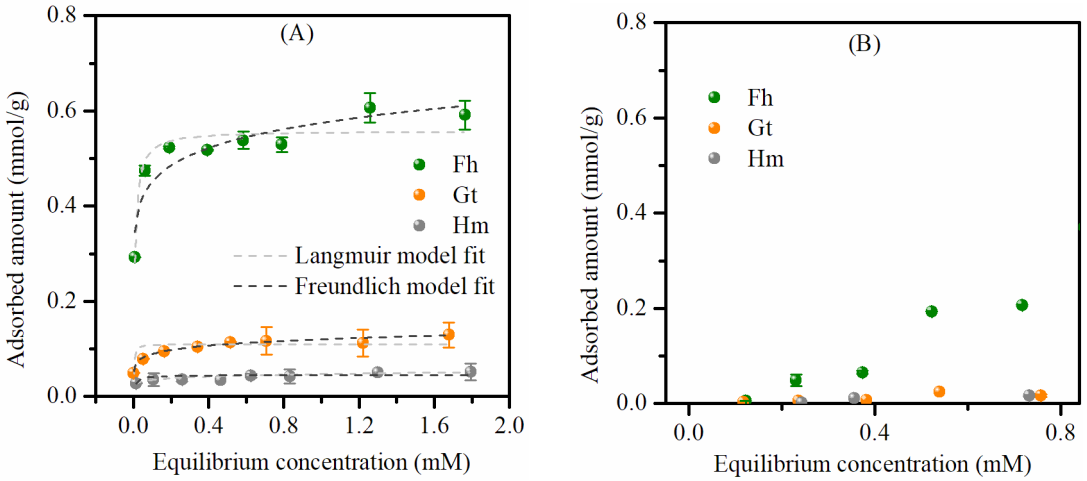

Fig. S3. Synchronous (the figures filled with the red) and asynchronous spectra (the figures filled with red and blue) of phosphate complexes on goethite in the binary (A) and ternary adsorption systems (B).

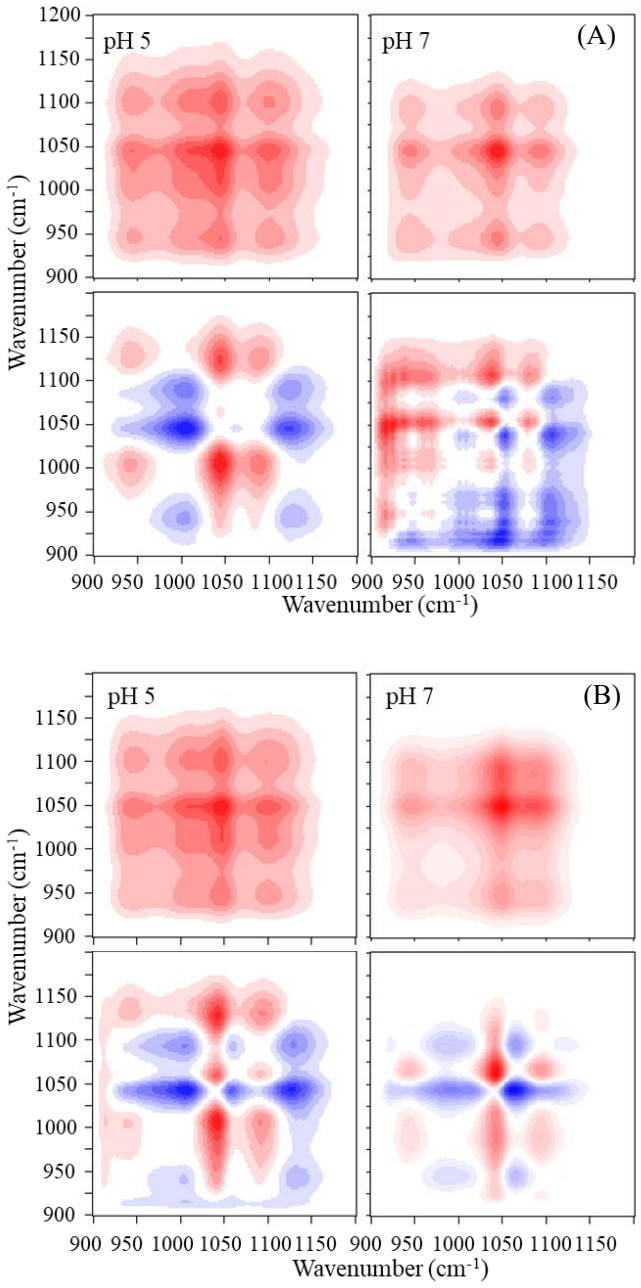


The spectra of phosphate complexes adsorbed on goethite show intense noise at frequencies below 960 $cm^{-1}$, possibly due to the vibration of the mineral and hence the peaks below 960 $cm^{-1}$ will not be discussed in the goethite systems. The synchronous and asynchronous spectra in different systems are similar. All of the synchronous spectra display the synchronous correlation between three peaks: 1100, 1044, and

(947) $cm^{-1}$, suggesting the dominance of this phosphate species on goethite. The asynchronous spectra indicate another set of peaks at ~1125, 1055, and 1000 $cm^{-1}$. Previous studies suggested that the frequency at 1120 $cm^{-1}$ representing $\nu$(P=O) and the frequency at 1008 $cm^{-1}$ representing $\nu_{as}$(P-$(OFe)_2$ belonged to the monoprotonated bridging bidentate complex. As the peak at 1055 $cm^{-1}$ is very close to that at 1044 $cm^{-1}$, the signal might be a result of the distortion caused by the change of background during the test.

Fig. S4. Synchronous and asynchronous spectra of hematite in the binary (A) and ternary adsorption systems (B).

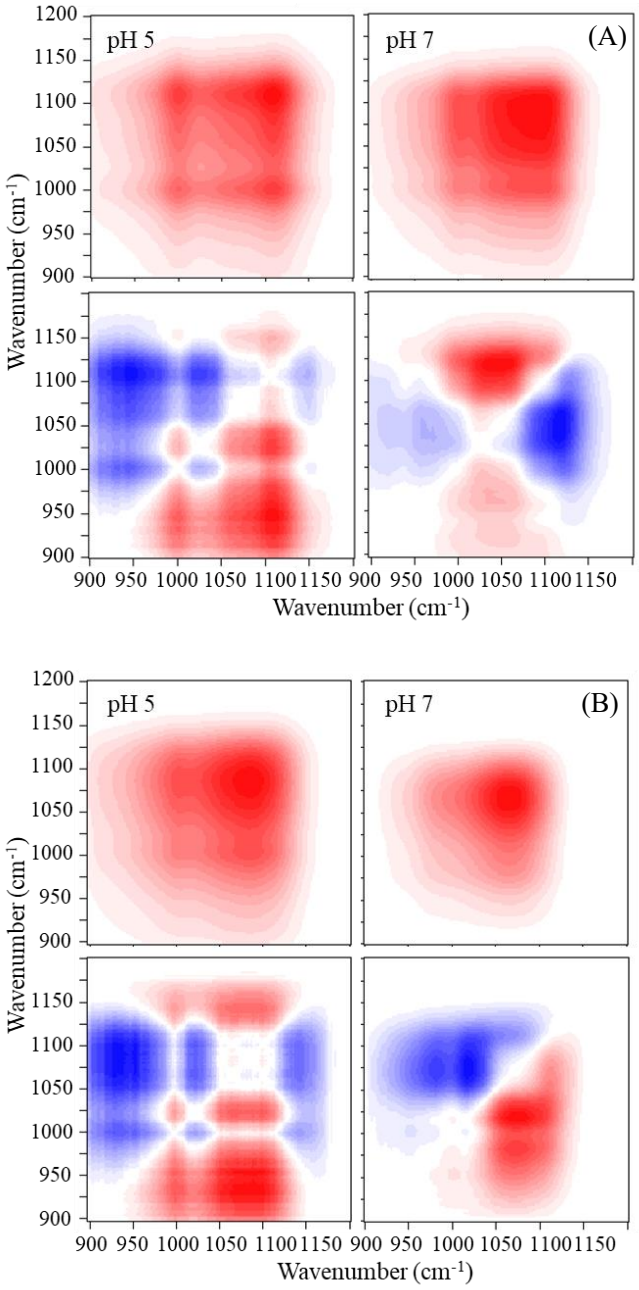


The synchronous and asynchronous spectra of the phosphate species on hematite under various conditions reveals similar bands. The synchronous spectra suggest synchronous correlation between the two peaks at 1120 and 1000 $cm^{-1}$; on the other hand, synchronous spectra indicate that the peak at 1120 $cm^{-1}$ had asynchronous signals with the peaks at 1040 and 1085 $cm^{-1}$; meanwhile, the peak at 1040 $cm^{-1}$ had asynchronous signals with the peaks at 1000 and 1120 $cm^{-1}$. Hence, two classes of

peaks could be identified: peaks at 1120 and 1000 $cm^{-1}$ belong to one species, and the peaks at 1085 and 1040 $cm^{-1}$ were the vibrations of the other complexes. The signals of the $\nu_1$ vibrations at 965 and 935 $cm^{-1}$ were not clear in the 2D plots. Hence, they were classified according to the deconvolution results. As the peak at 935 $cm^{-1}$ grew synchronously with the first species and the peak at 965 $cm^{-1}$ was synchronous with the other, the two $C_{2v}$ species (the species with peaks at 1120, 1000, and 935 $cm^{-1}$ and the species with peaks at 1085, 1040, and 965 $cm^{-1}$) were identified.

Fig. S5. Synchronous and asynchronous spectra of phosphate on ferrihydrite in the binary (A) and ternary adsorption systems (B).

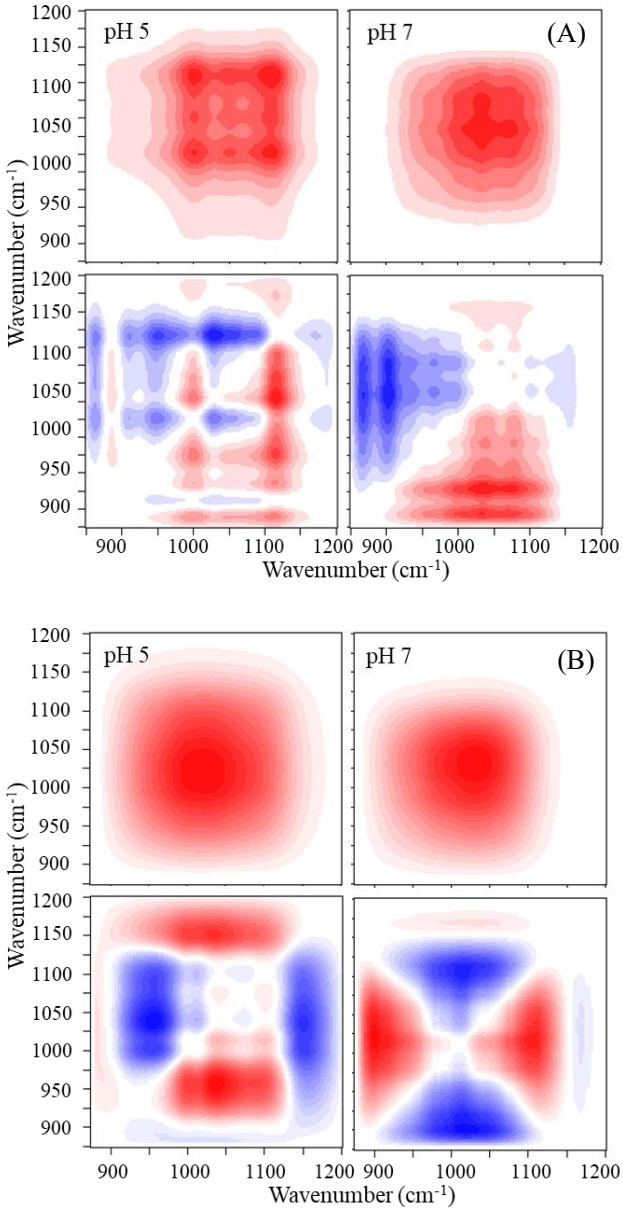


The different contributions of each complex to the phosphate adsorption result in varied 2D contour plots at different conditions. In the single solute adsorption system at pH 5, peaks at 1110, 1078, 1050, 1028, 992, and 952 $cm^{-1}$ could be recognized according to the synchronous and asynchronous plots. Much useful information could be got from the plots: the peak at 1110 $cm^{-1}$ shows synchronous signal with the peak at 992 $cm^{-1}$, while displays asynchronous signals with 1028 and 952 $cm^{-1}$; peaks at 1078 and 1028 $cm^{-1}$ have synchronous signal; 1028 $cm^{-1}$ have asynchronous signal

with peak at 992 $cm^{-1}$; peak at 992 $cm^{-1}$ have asynchronous signal with peak at 952 $cm^{-1}$. Based on this information, two adsorbed phosphate species could be recognized, species A with peaks at 1110, 1028, and 992 $cm^{-1}$ and species B with peaks at 1078, 1050, and 952 $cm^{-1}$. At pH 7, two classes of peaks can be recognized using the same method: 1100 and 970 $cm^{-1}$ for $C_{3v}$ species, and 1075, 1035, 945 $cm^{-1}$ for $C_{2v}$ species.

In the simultaneous adsorption systems, peaks at 1128, 1100, 1080, 1045, 1010, 979, and 945 $cm^{-1}$ could be recognized, suggesting possible three species co-existed on Fh surfaces. Two species that are similar to those formed on goethite and hematite could be identified: species with peaks at 1128, 1010, and 945 $cm^{-1}$ and the species with vibrations at 1080, 1045, 979 $cm^{-1}$.